

Sensors

Electrospun Nanofibers from a Tricyanofuran-Based Molecular Switch for Colorimetric Recognition of Ammonia Gas

Tawfik A. Khattab,^[b] Sherif Abdelmoez,^[b] and Thomas M. Klapötke*^[a]

Abstract: A chromophore based on tricyanofuran (TCF) with a hydrazone (H) recognition moiety was developed. Its molecular-switching performance is reversible and has differential sensitivity towards aqueous ammonia at comparable concentrations. Nanofibers were fabricated from the TCF–H chromophore by electrospinning. The film fabricated from these nanofibers functions as a solid-state optical chemosensor for probing ammonia vapor. Recognition of ammonia vapor occurs by proton transfer from the hydrazone fragment of the chromophore to the ammonia nitrogen atom

and is facilitated by the strongly electron withdrawing TCF fragment. The TCF–H chromophore was added to a solution of poly(acrylic acid), which was electrospun to obtain a nanofibrous sensor device. The morphology of the nanofibrous sensor was determined by SEM, which showed that nanofibers with a diameter range of 200–450 nm formed a nonwoven mat. The resultant nanofibrous sensor showed very good sensitivity in ammonia-vapor detection. Furthermore, very good reversibility and short response time were also observed.

Introduction

Alkaline gases are defined by their ability to increase the pH value of an aqueous phase above 7. Ammonia is the technologically most important example of such gases.^[1,2] The detection of ammonia is of special interest because of both the comparatively high toxicity of ammonia and its huge technical turnover as an intermediate in the production of artificial fertilizers, polymers, textiles, and explosives. Pure ammonia even finds application as a refrigerating agent.^[3–10] Being able to establish the concentration of ammonia both in gases and in the aqueous phase is of interest in many fields, such as the food industry, medical diagnosis, electronic device processing, ecology, and quality control.^[6–13] A sensitive and fast method for the determination of ammonia is required because of its detrimental effects to human health at low concentrations. Exposure to ammonia gas at levels higher than 1 ppm may cause nose, eye, and throat irritation. Above 25 ppm, intense burning of the skin and eyes and permanent damage to the lungs can occur, and exposure to 300 ppm is absolutely life-threatening. Furthermore, the maximum value allowed in the work place for a total of 8 h exposure is only 25 ppm, but the olfactory limit for the detection of ammonia gas is 55 ppm. Ammonia is

also flammable at concentrations of approximately 15–28 vol% in air.^[14–17] Hence, various sensor materials have been developed for the detection of ammonia, such as tellurium thin films,^[18] nanoporous anodized alumina,^[19] CuBr thin films,^[20] acrylic-acid-doped polyaniline,^[21] solid-state CuS films,^[22] and Langmuir–Blodgett polypyrrole films.^[23] However, the sensors prepared with the above sensing materials have a limit for ammonia detection below the ppm level, that is, they are not sensitive enough. Furthermore, these sensing materials are often slow, irreversible, or necessitate high operating temperatures.^[15,16,24,25]

The development of new approaches toward highly sensitive detection techniques, particularly at the ppb level, remains a major challenge in the field of chemical sensing. The detection of ammonia by means of a sensitive surface is attractive because of the possible accumulation by adsorption. As a consequence, the sensitivity of such a sensor is enhanced by increasing the surface area of the material of the detector. Modern electrospinning would be an attractive method for the generation of materials even on an industrial scale with well-defined large inner surfaces where fast response and gas exchange can be expected. Moreover, nanofibers obtained by such a process may form a mechanically stable tissue with expected long running life. Electrospinning is a process by which high static voltages are used to produce an interconnected membranelike web of small fibers with diameters in the range of 10–1000 nm. This technique can be used with a variety of polymers along with an active ingredient to produce nanoscale fibrous membranes.^[24,26,27] Electrospun nanofibrous membranes can have approximately 1–2 orders of magnitude more surface area than is found in continuous thin films, which makes them excellent candidates for providing much higher sensitivity and shorter response time in sensing applications.

[a] Prof. Dr. T. M. Klapötke
Department of Chemistry Energetic Materials Research
Ludwig Maximilian University
Butenandtstrasse 5–13
81377 München (Germany)
Fax: (+49) 89-2180-77492
E-mail: tmk@cup.uni-muenchen.de

[b] Dr. T. A. Khattab, Dr. S. Abdelmoez
Dyeing, Printing and Auxiliaries Department
Textile Research Division National Research Centre Dokki
Cairo 12311 (Egypt)

The large surface area-to-volume ratio of the nanofibers and their porous nature result in fast diffusion through the mesh and adsorption onto the surface of the nanofibers.^[28]

Herein, we report on a simple method for the preparation of a reversible sensor that is composed of hydrazone (H) donor and tricyanofuran (TCF) acceptor moieties (Figure 1) as optical

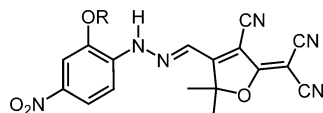


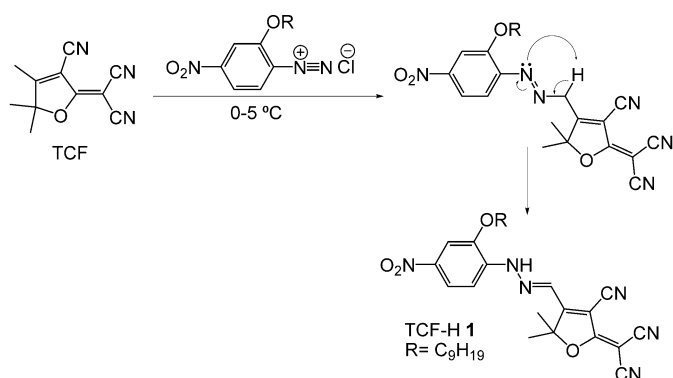
Figure 1. TCF-H molecular switch 1; R = C₉H₁₉

molecular-switching probe. In a push-pull system, the deprotonated hydrazone group can function as a bridge between donor and acceptor fragments, or itself function as a donor fragment in conjugation with a strongly electron withdrawing group.^[29] The electrospinning process can produce tunable nanofibers as a solid-state sensing device, which can be used like a test paper. SEM is used to study the properties of the resulting nanoscale structures. Due to the increased surface-to-volume ratio, the miniaturized solid-state film that is formed exhibits high sensitivity on exposure to ammonia gas. The characteristics and analytical performance of the sensor, including its reversibility and detection limits, are described. In addition, the response of the TCF-H chromophore to aqueous ammonia in homogenous solution was investigated.

Results and Discussion

Synthesis and characterization of TCF-H chromophore 1

Stimuli-responsive materials are important because they can potentially afford smart materials that can be applied in a variety of applications from nanotechnology to pharmacology. Molecular switches can undergo molecular-structure changes in response to external physical or chemical stimuli such as light, pH, and chemical agents. Hydrazone-based molecular switches are characterized by their modularity, stability, and simple preparation. Hence, hydrazones can be employed for various medicinal and supramolecular purposes.^[29] The hydrazone structural unit is related to the structure of ketones and aldehydes by replacing the oxygen atom with a =N-NH- group. Hydrazones can be used for molecular switching since they contain an imine group that can undergo stimuli-responsive *cis/trans* isomerization and/or also have the ability to lose a proton (Brønsted acid).^[29] The simple synthetic approach used for the preparation of TCF-H sensor 1 is shown in Scheme 1. The TCF intermediate was prepared in a 68% yield according to an early literature method.^[30] The starting material 2-amino-5-nitrophenol is commercially available and was treated with K₂CO₃ and 1-iodononane in dimethylformamide at reflux to afford 2-nonyloxy-4-nitrobenzenamine in a relatively high yield of 83%.^[31] The hydrogen atoms located on a carbon atom adjacent to a highly electron withdrawing group in a mol-



Scheme 1. Synthesis of the hydrazone-tricyanofuran donor-acceptor chromophore; R = C₉H₁₉

ecule are considerably more acidic those on a carbon atom that is adjacent to alkyl units. Here, the electron-withdrawing cyano groups of the TCF fragment help to stabilize the carbanion that is produced by removal of a proton from the activated methyl group. The hydrazone moiety of the TCF chromophore acts as a signal switcher, which is designed to switch on when the hydrogen atom on the NH group is abstracted to form a hydrazone anion that shows extended conjugation. In the TCF-H anion, the TCF fragment acts as an electron acceptor, and the hydrazone anion moiety as an electron donor. The presence of the NH group in the hydrazone form 1 inhibits internal charge transfer between the TCF moiety and the lone pair of electrons on the nitrogen atom of the NH group. The synthetic route is simple and involves azo coupling starting from tricyanofuran and 2-nonyloxy-4-nitrobenzenamine diazonium chloride. The azo coupling process is a base-mediated reaction between the diazonium salt and the TCF, which bears an active methyl group, to afford the corresponding unstable azo form, which transforms directly into the more stable hydrazone form.^[32] The structure of 1 was characterized by ¹H and ¹³C NMR spectroscopy, elemental analysis (C, H, N), and FTIR spectroscopy.

Photophysical properties of chromophore 1 in solution

The optical properties of chromophore 1 in polar and nonpolar organic solvents are shown in Table 1 and Figure 2. The color of 1 in various solvents ranges from yellow to purple. Generally, the main absorption peak shows a bathochromic shift (positive solvatochromism) with increasing solvent polarity (ca. 38 nm shift on going from chloroform to DMSO) and diverse intensities. These features indicate a strongly allowed π - π^* transition with charge-transfer character.

The 4-nitrophenylhydrazone fragment can function as a donor fragment that, in conjugation with the strongly electron withdrawing group, results in the formation of a stable push-pull system. The strongly electron withdrawing nitro group facilitates the generation of a hydrazone anion. Hence, distinct solvatochromic activities were observed in polar protic and aprotic solvents. In protic solvents, a discernible blueshift was observed due to the increased acidity of the alcohol sol-

Table 1. Variation of the λ_{\max} values of sensor 1 in various solvents.			
Solvent	$E_r(30)^{[33]}$ [kcal mol ⁻¹]	λ_{\max} [nm]	
		Abs.	Em.
methanol	55.4	484	531
ethanol	51.9	487	534
<i>n</i> -propanol	50.7	488	536
acetonitrile	45.6	477	539
DMSO	45.1	496	557
dichloromethane	40.7	472	538
chloroform	39.1	469	537
THF	37.4	476	535
1,4-dioxane	36.0	478	532
toluene	33.9	478	531

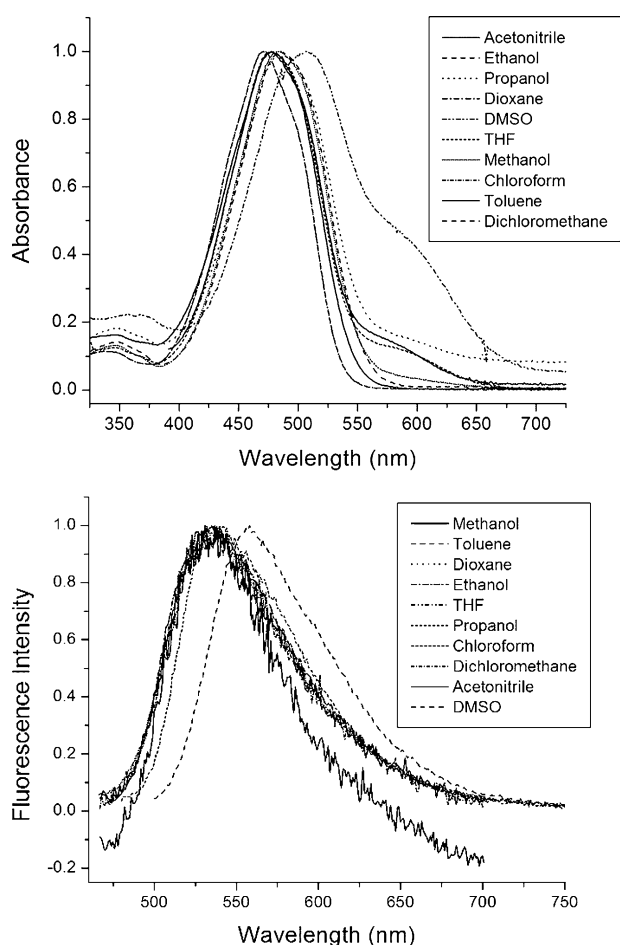


Figure 2. UV/Vis absorption (top) and fluorescence emission (bottom) spectra of sensor 1 in various solvents.

vent. In aprotic solvents, the λ_{\max} values for a given dye are generally larger than those in alcohol solvents with little consistency in the variation of the transition energy with the polarity of the medium.

Optical properties of TCF-H as ammonia sensor

The presence of ammonia in solution affects the pH of the medium. Therefore, the interaction of the TCF-H sensory chro-

mophore with ammonia in organic solutions was investigated. The UV/Vis absorption spectra of 1 were monitored on the addition of increasing concentrations of ammonia by using a methanolic solution of aqueous ammonia (Figure 3). The

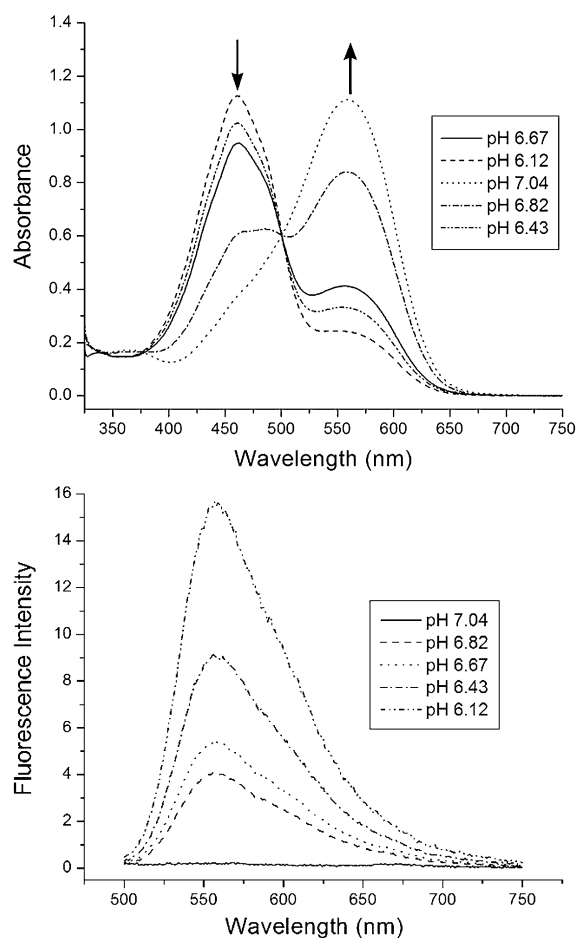
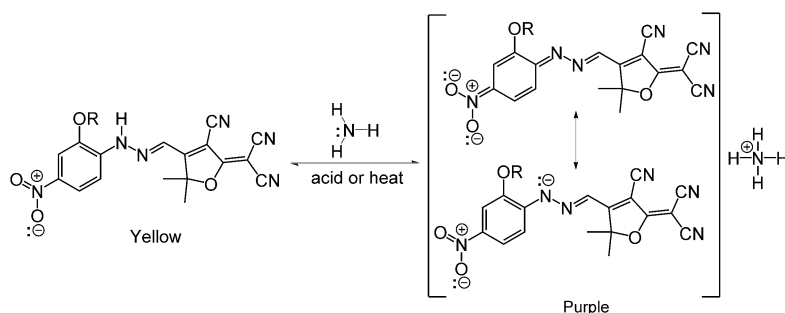


Figure 3. UV/Vis absorption (top), and fluorescence emission (bottom) spectra of TCF-H ($c \approx 1.6 \times 10^{-7}$) in acetonitrile on addition of increasing concentrations of a methanolic solution of aqueous ammonia.

gradual addition of aqueous ammonia results in an increase in the pH value from 6.12 to 6.43, 6.67, 6.82, and 7.04 with color changes from yellow to orange, red, violet, and purple, respectively. On reaction with ammonia, the hydrazone NH group is reversibly converted to a hydrazone anion by deprotonation (Scheme 2). This acid-base reaction is accompanied by an increase in the electron-donating effect of the hydrazone anion group, which results in a change in the electron delocalization within the chromophore molecule, and therefore the absorption maxima corresponding to the deprotonated molecule is shifted to longer wavelengths.

The stepwise addition of a methanolic solution of aqueous ammonia to a solution of 1 and subsequent recording of the corresponding absorption maxima λ_{\max} in acetonitrile led to a series of spectra and an isosbestic point at 502 nm. Due to formation of the hydrazone anion, the intensity of the absorption at shorter wavelength decreased, while simultaneously an



Scheme 2. Proposed mechanism for the colorimetric and fluorometric sensing of both gaseous and solution phases of ammonia.

absorption at longer wavelength appeared and increased in intensity. The resulting absorption spectra indicated a significant bathochromic shift between the neutral TCF-H and hydrazone anion derivative with increasing number of strongly electron-withdrawing nitro groups in the sensor dye. The fluorescence wavelength λ_{max} maxima of the sensor dye were recorded with stepwise addition of a methanolic solution of aqueous ammonia in a variety of solvents. In contrast to the pristine (protonated) TCF-H derivatives, the corresponding hydrazone anions did not show any fluorescence in the selected solvents. When the amount of methanolic solution of aqueous ammonia added to the dye solution is increased, the fluorescence intensity decreases in proportion, which indicates formation of the corresponding hydrazone anion.

We were able to construct a calibration curve for ammonia solutions in the concentration range 0–750 nM by measuring their UV/Vis absorption spectra. The TCF-H sensor was successfully applied to estimate the (unknown) concentration of ammonia in a solution. For example, the changes in the UV/Vis absorption spectra of TCF-H in acetonitrile solution on adding varying amounts of aqueous ammonia solution are shown in Figure 4.

The reversibility of the sensing effect towards ammonia in aqueous phase was monitored by warming the chromophore solution in the cuvette in situ from room temperature to 55 °C and maintaining it for a fixed time (5.0 min) to allow ammonia to evaporate. The UV/Vis electronic absorption and fluorescence emission spectra were recorded again after cooling to room temperature. The same amount of ammonia solution ($c = 1.1 \times 10^{-6} \text{ mol L}^{-1}$) was then added again to monitor the re-occurrence of the sensing. The changes in the ratio of the absorbances at 496 and 572 nm of TCF-H in DMSO solution ($c = 2.3 \times 10^{-5} \text{ mol L}^{-1}$) were recorded at ambient temperature. The absorbances of about 0.332 and 0.319 switched back and forth between 496 and 572 nm, respectively, on adding aqueous ammonia solution followed by heating. As is shown in Figure 5, at least for this many cycles, this process clearly exhibits high reversibility towards ammonia sensing without fatigue.

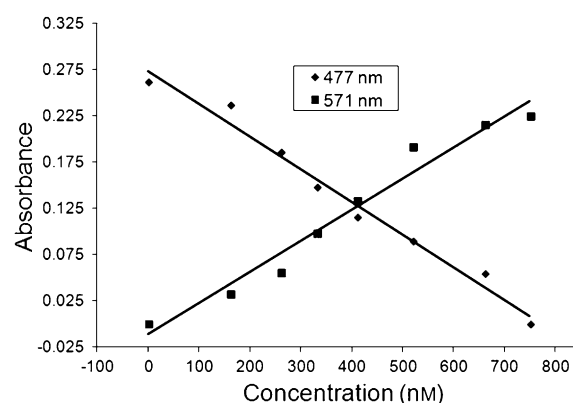


Figure 4. Changes in the UV/Vis absorption spectra of TCF-H in acetonitrile solution resulting from the addition of aqueous ammonia ($c = 0\text{--}750 \text{ nM}$). At 477 nm, $Y_1 = -0.0004X + 0.2728$, $R^2 = 0.981$; at 571 nm, $Y_2 = 0.0003X - 0.0113$, $R^2 = 0.9663$.

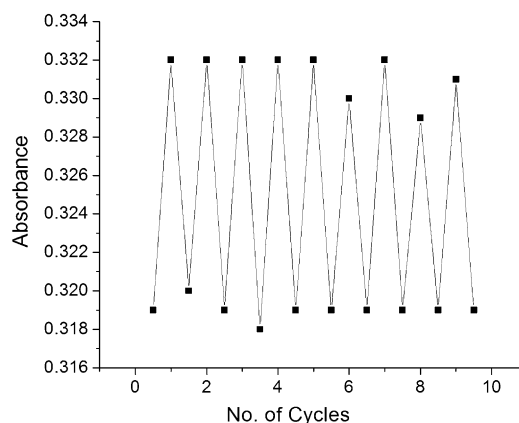


Figure 5. Changes in the ratio of the absorbance at 496 and 572 nm of TCF-H in DMSO solution ($c = 2.3 \times 10^{-5} \text{ mol L}^{-1}$) at ambient temperature.

Morphology of poly(acrylic acid)-TCF-H nanofibrous sensor

Solid-state sensor materials have some advantages, such as portability, operational simplicity, and reusability, which make rapid online detection possible at low cost.^[15,16] Thus it is very attractive, but also challenging, to develop solid-state optical sensor materials for direct detection of a trace target substance in both solution and vapor phases in real time. In terms

of practicability, a solid-state film sensor often has more favorable properties than a colorimetric probe dissolved in solution. The solid film probe may ultimately be employed in basic laboratory assays through portable devices and in household use as commercial indicators. Therefore, the quest for ecofriendly solid-film sensors with simple and smart detection is of great significance.^[15–18]

The electrospinning process used to produce the poly(acrylic acid) (PAA)–TCF–H nanofibers was developed by carrying out a series of systematic studies on the effects of flow rate, polymer and dye concentration, applied voltage, and needle tip-to-receiver distance on the spinnability and morphology of the polymer fibers. The concentration of TCF–H influences the sensitivity of the final fibrous sensor device. The best concentration of TCF–H for the preparation of cross-linked PAA–TCF–H nanofibrous sensor is 1.0 wt%. Increasing the amount of TCF–H to greater than 1.0 wt% leads to decreased sensitivity of the final fibrous sensor device. On the other hand, no color change was detected on decreasing the amount of TCF–H to less than 1.0 wt%. Electrospinning is an efficient, relatively simple, and low-cost way to produce polymer and composite fibers with diameters ranging from several micrometers to a few nanometers by applying a high voltage to a polymer solution or melt ejected from a microsyringe pump. Porous three-dimensional membranes assembled from electrospun fibers generally show large specific surface area, high porosity, and good interconnectivity. These features of electrospun fibrous membranes result in their potential application in ultrasensitive and highly miniaturized sensors. An SEM image of a pure PAA–TCF–H nanofibrous sensor is shown in Figure 6. The nanofibers with a diameter of 200–450 nm (average diameter of the nanofibers is ca. 325 nm) formed a nonwoven mat with a porous three-dimensional structure, and the addition of TCF–H did not affect the morphology of the nanofibrous sensor. The resulting PAA–TCF–H nanofibrous sensor shows a porous 3D structure with random fiber orientation and great potential as a sensor for applications. The thinner solid-state

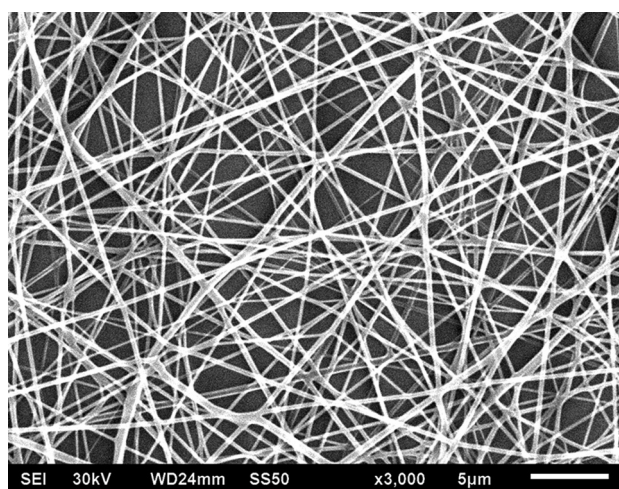


Figure 6. SEM image of electrospun fibers of the PAA–TCF–H composite, which can be used for solid-state reversible optical sensing of ammonia in the gas phase.

nanofibers exhibit higher sensitivity with respect to the detection of ammonia gas due to the higher surface-to-volume ratio and larger interspaced network, which enables the diffusion of guest ammonia through the matrix.

The solid-state film samples were exposed to ammonia gas and showed an instant color change from orange to blue, which was monitored with the naked eye. On removal of the film sensor from the ammonia gas, the sample quickly recovered its original orange color as the ammonia concentration decreased. The sensor could be used repeatedly without any apparent degradation. To test the film sensor, an aqueous ammonia solution (2 mL) was placed in a 4 mL glass vial. After generating saturated ammonia vapor, the nanostructure-based film was placed near the top of the vial and showed an instant and reversible color change without fatigue (see video abstract).

Conclusion

We have developed a PAA–TCF–H nanofibrous sensor for ammonia sensing by electrospinning. The TCF–H sensor can detect ammonia at the ppb level in solution phase. The ammonia sensing is reversible and the nanofibrous sensor can be reused several times. Compared to small-molecule chemosensors, this nanofibrous sensor may represent a simple and expedient technique for practical detection in both solution and gaseous phases. The nanostructure aggregates of TCF–H exhibit solid-state optical sensing of ammonia vapor. Exposure to ammonia vapor resulted in a change of the observed color towards purple. The nanofibrous sensor shows very good sensitivity. In addition, this reusable nanofibrous solid-state sensor can be easily employed to enable practical sensing of aqueous ammonia, just like using a test paper.

Experimental Section

Materials and methods

Melting points were determined with an electrothermal melting point apparatus. IR spectra were recorded with a Bruker Vectra-33 IR spectrometer with a diamond ATR probe. Elemental analyses (C, H, N) were performed with PerkinElmer 2400 analyzer (PerkinElmer, Norwalk, CT, USA) at the Microanalytical Center, Cairo University. UV/Vis absorption spectra were measured with an HP-8453 spectrophotometer. Fluorescence spectra were measured with a VARIAN CARY ECLIPSE spectrophotofluorimeter. NMR spectra were recorded with a Bruker AVANCE 400 spectrometer at 400 MHz; chemical shifts are given in parts per million (ppm) relative to the internal standard TMS at 295 K. The morphology of the electrospun sample was examined with a Quanta 250 FEG scanning electron microscope operating at 30 kV. The SEM samples were coated with a layer of gold in vacuum by using an Edwards S150A sputter coater. Fiber diameters were measured by using the Image J software of the scanning electron microscope. For fluorescence emission and UV/Vis absorption measurements on solid fibers, the nanofibrous sensor was subjected to ammonia vapor evolved from aqueous ammonia solution for 10 min, washed with methanol and water, and dried with nitrogen, after which fluorescence emission and UV/Vis absorption measurements were con-

ducted. For investigating the reversibility (reusability) of the nanofibrous sensor, after exposure to ammonia vapor evolved from aqueous ammonia solution for 10 min, the nanofibrous sensor was washed with methanol and water and dried under nitrogen. Fluorescence emission and UV/Vis absorption measurements were then conducted. The photographs of the nanofibrous sensor before and after sensing of ammonia vapors evolved from aqueous ammonia solution were taken by a Canon Power Shot A710 IS digital camera. Solvents used in this study were obtained from Fluka and Aldrich. All reactions were monitored by TLC on Merck aluminum plates precoated with silica gel PF254, 20–20, 0.25 mm, and detected by visualization of the plate under a UV lamp (254 or 365 nm). Compounds were purified by recrystallization or flash column chromatography on Scharlau silica gel, packed by the slurry method.

Electrospinning apparatus

A typical electrospinning device has three main components: power supply, polymer-solution delivery system, and collector. Briefly, a programmable syringe pump was used to deliver polymer solutions at controlled flow rates. The polymer solution was given an electric potential that exceeds its forces of surface tension through the high voltage (0–30 kV) power supply. Consequently, a thin polymer fiber is ejected from the syringe needle (18 gauge, 1.27 mm) towards the collector, which results in ultrathin fibers being deposited on an aluminum foil of dimensions 10×10 cm. The aluminum foil was placed in the center of a piece of wood (15×15 cm), which was attached to a copper cylinder connected to the grounded cable. The polymer solution was filled into a plastic syringe with a stainless steel blunt needle tip connected to the dc voltage source. The height of the needle tip was adjusted to face and align with the center of the vertically oriented aluminum foil. The distance between the needle tip and collector (air-gap distance) was varied from 5 to 25 cm. All experiments were carried out in ventilated fume cupboard made of wood at room temperature.

Preparation of PAA–TCF–H electrospun nanofibrous sensor

Cross linked PAA–TCF–H nanofibrous sensors were prepared as follows: Firstly, an ethanolic solution with 1 wt% TCF-H, 4 wt% PAA, and 16 wt% ethylene glycol was prepared by stirring at room temperature for 12 h until a homogeneous solution formed. Secondly, 1 drop of 1 M H₂SO₄ per milliliter of solution was added. The solution was then used for the electrospinning experiment. Typical parameters for electrospinning were as follows: the applied electric voltage was 30 kV, the solution feed rate was 0.8 mL h⁻¹, and the distance between the spinneret and the collector (a grounded metallic drum) was 20 cm. The grounded rotating metallic drum with diameter of 10 cm and length of 30 cm was used to collect the deposited nanofibers at a rotating speed of 180 rpm. The resulting nanofibrous sensor was dried in a vacuum oven at 40 °C until constant mass was achieved, and was then kept in a closed drybox before use.

Sensor testing

Aqueous ammonia (≈2 mL) was placed in a 4 mL glass vial. A glass slide with the PAA–TCF–H nanostructure-based film was placed near the top of the vial and showed an instant color change. The reversibility of the sensing effect was monitored by observing λ_{max} in the UV/Vis absorption spectra at 496 and 572 nm for the TCF–H chromophore in DMSO solution (c=2.3×10⁻⁵ mol L⁻¹) at ambient temperature. The absorption spectra were

switched back and forth between 496 and 572 nm by adding aqueous ammonia solution (c=1.1×10⁻⁶ mol L⁻¹) and recording the absorption spectra. This was followed by raising the temperature of the cuvette inside the spectrophotofluorimeter from room temperature to 55 °C and maintaining it for a fixed time (5.0 min) to allow the ammonia to completely evaporate. The UV/Vis absorption spectra were recorded again after cooling to room temperature. The same amount of ammonia solution was added again to monitor whether sensing occurred again.

Synthesis of 2-(dicyanomethylene)-2,5-dihydro-4-[methyl-(2-nonyloxy-4-nitro-phenylazo)]-5,5-trimethylfuran-3-carbonitrile (1)^[32]

A mixture of 4-nitro-2-nonyloxy-4-nitrobenzenamine (1.1 g, 4.0 mmol), hydrochloric acid (3.0 mL), and water (2.0 mL) in a 25 mL Erlenmeyer flask was stirred and cooled in an ice bath at 0–5 °C. The aniline diazonium salt was prepared by slow addition of a solution of sodium nitrite (345 mg, 5.0 mmol) in water (3.0 mL) at 0–5 °C. The resulting mixture was stirred for a further 20 min at 0–5 °C. In a separate round-bottom flask, tricyanofuran (800 mg, 4.0 mmol) was dissolved in acetonitrile (7.0 mL), the solution was cooled to 0–5 °C, and acetic acid (2.5 mL) and sodium acetate (3.0 g) were added. This mixture was vigorously stirred in the ice bath at 0–5 °C while the cold solution of diazonium salt was added dropwise. After stirring the resulting mixture for a further 2 h, the crude solid product was filtered off with a Buchner funnel, washed with distilled water (3×15 mL), crystallized from toluene/ethanol, and air-dried to afford a red solid (1.41 g, 73% yield); m.p. 198–200 °C; ¹H NMR (400 MHz, CDCl₃): δ = 9.68 (s, 1H, NH), 8.02 (s, 1H, =CH), 7.98 (dd, 1H, J = 8.8 Hz, 2.0 Hz), 7.83 (s, 1H, J = 2.4 Hz), 7.43 (d, 1H, J = 9.2 Hz), 4.22 (t, 2H, J = 6.8 Hz), 1.97 (m, 2H), 1.91 (s, 6H), 1.53 (m, 2H), 1.36 (m, 10H), 0.91 ppm (t, 3H, J = 4.0 Hz); ¹³C NMR (400 MHz, CDCl₃): δ = 175.26, 170.65, 145.85, 143.79, 135.75, 128.82, 118.04, 112.95, 111.52, 111.12, 109.66, 107.33, 100.26, 98.60, 70.00, 57.92, 31.91, 29.65, 29.57, 29.35, 26.77, 25.93, 22.69, 14.13 ppm; IR (neat): ν̄ = 3274 (NH), 2231 (CN), 1592 (C=N), 1532, 1332 cm⁻¹ (NO₂); elemental analysis calcd for C₂₆H₃₀N₆O₄ (490.23): C 63.66, H 6.16, N 17.13; found: C 63.57, H 6.12, N 17.03.

Acknowledgements

We gratefully acknowledge National Research Center, Cairo for the support of this work.

Keywords: ammonia · colorimetry · electrospinning · nanostructures · sensors

- [1] B. S. Hobbs, Y. S. Chan, U. S. Patent, **1993**, 5,234,567, issued August 10.
- [2] C.-J. Tsai, C.-H. Huang, S.-H. Wang, T.-S. Shih, *Environ. Sci. Technol.* **2001**, *35*, 2572–2575.
- [3] O. Braissant, *Mol. Genet. Metab.* **2010**, *100*, S53–S58.
- [4] V. Walker, *Diabetes Obes. Metab.* **2009**, *11*, 823–835.
- [5] D. Häussinger, B. Görg, *Curr. Opin. Clin. Nutr. Metab. Care* **2010**, *13*, 87–92.
- [6] E. Wessén, K. Nyberg, J. K. Jansson, S. Hallin, *Applied Soil Ecology* **2010**, *45*, 193–200.
- [7] J. Singh, A. Kunhikrishnan, N. S. Bolan, S. Sagggar, *Sci. Total Environ.* **2013**, *465*, 56–63.
- [8] V. R. Dayeh, K. Schirmer, N. C. Bols, *ATLA Altern. Lab. Anim.* **2009**, *37*, 77–87.
- [9] Z. Tamainot-Telto, S. J. Metcalf, R. E. Critoph, Y. Zhong, R. Thorpe, *Int. J. Refrig.* **2009**, *32*, 1212–1229.

- [10] K. Kafle, K. Greeson, C. Lee, S.H. Kim, *Text. Res. J.* **2014**, 0040517514527379.
- [11] K. Ruland, A. Fischer, K. Hartmann, *Veterinary Clinical Pathology* **2010**, 39, 57–64.
- [12] T.S. Almeida, K. Coutinho, B. J. Costa Cabral, S. Canuto, *J. Chem. Phys.* **2008**, 128, 014506.
- [13] K. Aika, L. J. Christiansen, I. Dybkjaer, J. B. Hansen, P. E. Hojlund Nielsen, A. Nielsen, P. Stoltze, K. Tamaru, *Ammonia: catalysis and manufacture* (Ed.: A. Nielsen), Springer Science & Business Media, **2012**.
- [14] P. Gouma, K. Kalyanasundaram, X. Yun, M. Stanačević, L. Wang, *Sensors Journal IEEE* **2010**, 10, 49–53.
- [15] X. Ma, G. Li, M. Wang, Y. Cheng, R. Bai, H. Chen, *Chem. Eur. J.* **2006**, 12, 3254–3260.
- [16] M. P. Fraser, G. R. Cass, *Environ. Sci. Technol.* **1998**, 32, 1053–1057.
- [17] J. Manne, W. Jäger, J. Tulip, *Appl. Phys. B* **2009**, 94, 337–344.
- [18] S. Sen, K. P. Muthe, N. Joshi, S. C. Gadkari, S. K. Gupta, M. Roy, S. K. Deshpande, J. V. Yakhmi, *Sens. Actuators B* **2004**, 98, 154–159.
- [19] Y. Peng, D.-H. Qin, R.-J. Zhou, H.-L. Li, *J. Mater. Sci. Eng. B* **2000**, 77, 246–249.
- [20] P. Lauque, M. Bendahan, J.-L. Seguin, K. An Ngo, P. Knauth, *Anal. Chim. Acta* **2004**, 515, 279–284.
- [21] S. Virji, J. Huang, R. B. Kaner, B. H. Weiller, *Nano Lett.* **2004**, 4, 491–496.
- [22] A. A. Sagade, R. Sharma, *Sens. Actuators B* **2008**, 133, 135–143.
- [23] M. Penza, E. Milella, F. Musio, M. B. Alba, G. Cassano, A. Quirini, *J. Mater. Sci. Eng. B* **1998**, 5, 255–258.
- [24] B. Ding, M. Yamazaki, S. Shiratori, *Sens. Actuators B* **2005**, 106, 477–483.
- [25] K. M. Manesh, A. I. Gopalan, K.-P. Lee, P. Santhosh, K.-D. Song, D.-D. Lee, *Nanotechnology IEEE Transactions on* **2007**, 6, 513–518.
- [26] Y. J. Pan, J. D. Xian, Q. F. Wei, W. M. Hung, C. Y. Lin, Y. H. Ho, C. T. Hsieh, *Adv. Mater. Res.* **2011**, 421, 23–26.
- [27] Y. Zhang, J. J. Kim, D. Chen, H. L. Tuller, G. C. Rutledge, *Adv. Funct. Mater.* **2014**, 24, 4005–4014.
- [28] X. Wang, C. Drew, S.-H. Lee, K. J. Senecal, J. Kumar, L. A. Samuelson, *Nano Lett.* **2002**, 2, 1273–1275.
- [29] F. Han, Y. Bao, Z. Yang, T. M. Fyles, J. Zhao, X. Peng, J. Fan, Y. Wu, S. Sun, *Chem. Eur. J.* **2007**, 13, 2880–2892.
- [30] M. C. Davis, A. P. Chafin, R. A. Hollins, L. C. Baldwin, E. D. Erickson, P. Zarras, E. C. Drury, *Synth. Commun.* **2004**, 34, 3419–3429.
- [31] B. Su, E. S. Diaz-Cruz, S. Landini, R. W. Brueggemeier, *J. Med. Chem.* **2006**, 49, 1413–1419.
- [32] T. A. Khattab, R. J. Twieg, Abstracts, 44th Central Regional Meeting of the American Chemical Society, MI, United States, **2013** May 15–17, CERM-224, American Chemical Society, Washington, CODEN:69RDRC.
- [33] C. Reichardt, *Chem. Rev.* **1994**, 94, 2319–2358.

Received: November 5, 2015

Published online on February 11, 2016